Pure Appl. Chem., Vol. 80, No. 11, pp. 2309–2326, 2008.
doi:10.1351/pac200880112309

Development of novel linear, block, and branched oligoelectrolytes and functionally targeting nanoparticles*

Alexander Zaichenko[1,‡], Natalya Mitina[1], Oleh Shevchuk[1], Katerina Rayevska[1], Volodymyr Lobaz[1], Taras Skorokhoda[1], and Rostyslav Stoika[2]

[1]Lviv Polytechnic National University, 12 S. Bandera Str., Lviv, 79013, Ukraine; [2]Institute of Cell Biology, National Academy of Sciences of Ukraine, Drahomanov Str., 14/16, 79005, Lviv, Ukraine

Abstract: The objective of the present study is development of novel surface-active block, comb-like, and branched copolymers with peroxide-containing chains, as well as derived functional luminescent and magnetic nanoparticles. The main experimental approaches are based on tailored synthesis of the oligoperoxide surfactants of desired structures and derived coordinating complexes of transitional and rare earth elements. Oligoperoxide-based synthesis of luminescent, magnetic, and other functional nanocomposites with controlled size distribution, functionality, reactivity, and biocompatibility is described. Developed methods provide combining the formation of polymeric, metal, and metal-oxide nanoparticles with irreversible modification of their surface by functional fragments capable of radical and other reactions, including binding of physiologically active substances. Novel nanoparticles were studied by chemical, colloidal-chemical, and rheological methods, X-ray diffraction technique, luminescent spectroscopy, and transmission and scanning electronic microscopy. The availability of ditertiary peroxide fragments on the nanoparticle surface provides a possibility of radical grafting functional polymer chains. The developed functional nanoparticles have been used for phagocytosis measurement, as well as markers of pathological cells, antimicrobial remedies, and nanocarriers for targeted drug delivery.

Keywords: nanoparticles; functional oligoperoxides; surface modification; luminescent labeling.

INTRODUCTION

The intense development of novel technologies of microelectronics, biochemistry, and medicine during the past few decades is based on targeted synthesis and use of a wide range of synthetic polymers with a high variety of chemical structure and properties. For example, the development of functional polymeric precursors is necessary for the design or improvement of microelectromechanical systems or their components [1,2], microphase-separated block copolymer thin films have emerged as a promising new technique for the creation of submicron/suboptical masks in the next generation of semiconductor and

*Paper based on a presentation at the 3rd International Symposium on Novel Materials and Their Synthesis (NMS-III) and the 17th International Symposium on Fine Chemistry and Functional Polymers (FCFP-XVII), 17–21 October 2007, Shanghai, China. Other presentations are published in this issue, pp. 2231–2563.

‡Corresponding author: E-mail: zaichenk@polynet.lviv.ua

magnetic media [3–5]. Dendrimers are being used as carrier molecules for drug delivery and gene transfer, as well as cell transfection agents [6,7], catalysts in homogeneous catalysis, and as scaffolds to accomplish multivalent presentation of ligands with interesting biological applications [8].

Until recently, the technique of radical polymerization for obtaining functional macromolecules of comb-like, highly branched, or block structures was less advanced by comparison with methods of condensation and analogous transformations [9–11]. That is caused, firstly, by the indeterminacy of structure and chain length peculiar to polymers derivable by radical polymerization techniques. Since the synthesis of telechelic surface-active oligoperoxides (SAPs) and oligoperoxide metal complexes (OMCs) with side peroxide fragments allows controlling radical polymerization initiated by them [12,13], which provides a more realistic and very promising approach for obtaining block, comb-like, and branched polymers with the backbone and branches of predictable chain structure, length, polarity, and reactivity.

At the same time, the global influence of nanotechnologies on technical progress demands the creation of diverse organic and inorganic nanomaterials with a wide spectrum of properties for their functional application. These are elementary units of nanoelectronics and nanophotonics (semiconductor transistors and lasers, photo detectors, solar cells, different sensors), devices for information superdense recording, informational, computation technologies as well as nanolithography, nanoimprinting, nanochemistry, and nanocatalysis [14–19]. The development of novel nanoparticles and nanocomposites with polymeric shell—which provides their colloidal stability, biocompatibility, chemical targeted functionality and reactivity—is of significant value for obtaining nanoscale carriers and labels of biomedical application [20–22]. A variety of synthetic technologies for the preparation of nanoparticles of biomedical application with narrowed size distribution and tailored functionality and reactivity are available [20,21]. However, nanoparticle-targeted irreversible surface functionalization still remains among the main problems of particle synthesis and their biomedical application.

A brief review of principal approaches developed in our laboratory for tailored synthesis of SAPs and OMCs based on new functional polymeric, inorganic, and hybrid colloidal nanoparticles [23,24] is presented. The main techniques of sorption modification and/or polymerization and reactions of functional oligoperoxide surfactants predominantly for biomedical application are described.

MATERIALS AND METHODS

Monomers: vinyl acetate (VA), acrylic acid (AA), styrene (St), butyl acrylate (BA), *N*-vinylpyrrolidone (*N*-VP), and 2-*tert*-butylperoxy-5-methylhex-1-en-3-yne (VEP) were purified by vacuum distillation; glicydyl methacrylate (GMA, Merck) was used, as obtained; maleic anhydride (MAN) was purified by using sublimation technique.

Telogens: 1-(1-*tert*-butylperoxy-1-methylethyl)-4-isopropylbenzene (MP) was purified by vacuum distillation.

Initiators: coordinating OMCs were obtained by the reactions of SAP with copper chloride in methanol solution at ambient temperature and mild stirring (polymer:$CuCl_2$, w/w ratio 1:1), then precipitated with distilled water, filtered, and dried under vacuum. Luminescent initiators were obtained by using the same technique with rare-earth metal salts (Ce, Eu, Nd chlorides). 2,2'-Azobis(2-methylpropionitrile) (AIBN, Merck) was used, as obtained.

Solvents: Ethyl acetate, dioxane, toluene, methanol, and benzene were of analytical grade and used without additional purification.

Sample preparation

All polymerization reactions were performed in glass dilatometers under argon to control reaction kinetics and product yield. Synthesis conditions are presented in the discussion section. Obtained sam-

ples were twice re-precipitated from organic solvents and dried under vacuum. Vinyl alcohol fragments in polymer molecules were obtained by alkaline hydrolysis of VA links in methanol solution.

Nanoparticles of polystyrene and polyacrylates including luminescent ones were synthesized by water dispersion polymerization initiated by AIBN or functional OMC. Colored polymeric nanoparticles were obtained by incorporation of specific unsaturated dyes (MD) into the particles.

Reactive Ni colloids, Fe_3O_4, Ag, and other nanoparticles with narrowed particle size distribution and tailored functional shell and compatibility were synthesized by nucleation technique from water solutions of corresponding metal salts in the presence of SAP in the reaction mixture [25,26].

Sample characterization

The content of VEP and MP links was calculated taking into account volatile products of decomposition of peroxide groups detected by gas–liquid chromatograph (Selmi Chrom-1) according to [27].

Surface tension of water-ammonia solutions of polymers was measured by PPNL-1 device using the technique of excessive pressure in the vesicle.

Intrinsic viscosity [η] of polymer solutions was measured by using Bishoff viscosimeter, in acetone at 298 K. For homopolymers, viscosity-average molecular weight was calculated by using equation $[\eta] = KM^{\alpha}$ as referred K and α values [28].

UV–vis spectrometry was performed at SPECORD-40 (Germany).

The structure of the particle inorganic core and magnetite crystal size were determined taking into account the results of X-ray diffraction analysis data ("DRON-30", CoK_{α} irradiation) using the Scherrer equation.

Crystal size distribution was obtained from transmission electron microscopy (TEM) micrographs ("JEOL" JEM-200A, accelerating voltage, 200 kV) and small-angle X-ray scattering (SAXS) measurements using a Guinier plot of scattering intensity vs. scattering vector fluctuation.

Composite particle size was studied by scanning electron microscopy (SEM) (Akashi ISI DS 130C microscope).

The content of adsorbed SAP and grafted copolymer was determined by elemental analysis.

Opsonization of functional nanoparticles with specific proteins for phagocytosis was performed, as follows. Latex particles were pelleted by centrifugation, the pellet was washed twice with 0.1 M phosphate-buffered saline (PBS) (pH = 7.4), and suspended in double volume of human blood serum or 0.5 % solution of concanavalin A in the same buffer. The suspension of the nanoparticles was kept in refrigerator at 4 °C for 24 h, thereafter washed several times with PBS, and the final suspension was standardized according to the number of nanoparticles per ml (usually 400–500 mln/ml).

RESULTS AND DISCUSSION

Oligoperoxide-based initiators–precursors for block copolymerization were synthesized by telomerization of VA, AA, St, or their mixtures with BA and MAN in hydrocarbon media in the presence of peroxide-containing telogens.

Earlier, we [23] have shown that only one terminal peroxide-containing fragment of MP can be included in the polymeric structure, providing the availability of active radical-forming site in the molecule of polymer-precursor.

The characteristics of the kinetics of polymerization reaction (Table 1) shows that polymerization in the presence of peroxide-containing chain-transfer agents occurs at a feasible rate and yield and provides telechelic oligomers (TOs) of tailored structures. It is evident that the rate of polymerization, TO chain length, and peroxide functionality are determined by the telogen amount in the initial reaction system, as well as by the reaction conditions. One can see from the presented experimental data (Table 1) that MP is an effective chain-transfer agent possessing weakly inhibiting action which decreases polymerization rate value and lowers TO molecular weight at the increase of telogen concen-

tration. Moreover, the kinetic characteristics of the polymerization and the molecular weight and functionality of peroxide-containing oligomers depend on the nature and composition of the monomer system.

Table 1 Synthesis and characteristics of polymers with terminal peroxide fragments ([AIBN] = 10×10^{-3} mole/l, 333K).

Copolymerization					Polymerization rate $W \times 10^3$, %/s	Conversion, %	Polymer		
Monomers		Telogen	[T], %	Solvent			Telogen content in polymer, %	$M\eta \times 10^3$, g/mole	Number-average functionality f_n
VA		MP	5	In	1.5	68	0.16	18.0	0.13
VA		MP	20	block	0.37	62	3.25	8.00	1.17
VA		MP	30		0.11	59	3.80	6.80	1.16
VA	MA	MP	25	Ethyl	0.47	65	0.45	5.00	0.10
VA	MA	MP	33	acetate	0.13	65	4.00	4.00	0.72
VA	BA	MP	33		0.17	65	4.90	4.20	0.93

The presence of common absorption bands in the UV spectra of peroxide-containing telogens and oligomers with end MP fragment (Figs. 1 and 2) confirms entering of active telogen residue into the TO structure.

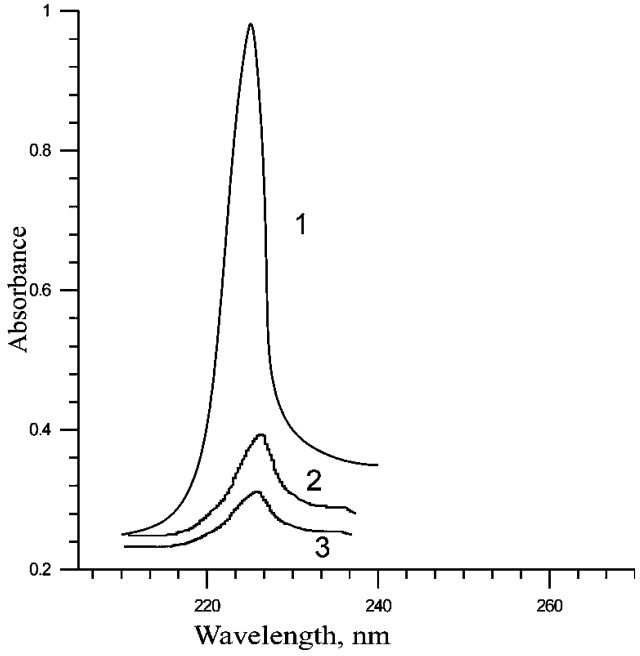

Fig. 1 UV spectra of: (1) MP; (2) poly VA-MP; (3) poly VA-BA-MP.

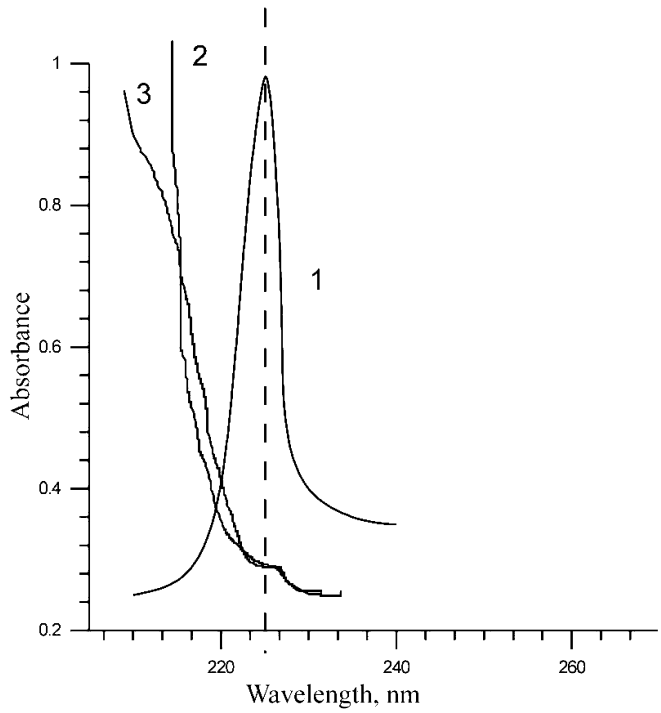

Fig. 2 UV spectra of block copolymers: (1) MP; (2) polyvinyl alcohol-St (M_n = 10 000 g/mole; (3) polyvinyl alcohol-BA (M_n = 8200 g/mole).

It is evident from Table 2, which represents the characteristics of synthesis and properties of obtained block copolymers, that MP-containing polymers are the active initiators of solution polymerization in various monomer systems. The initial polymeric initiators and resulting block copolymers possess different solubility and can be separated by dilution and precipitation in distinct solvents. The obtained block copolymers can be composed of blocks of different polarity containing various functional fragments including peroxide groups. The variation of synthesis conditions and the nature and concentration of both initial TO-initiator and monomer mixture provides a control of block copolymer chain length, hydrophilic–lipophilic balance (HLB), and reactivity.

Table 2 Synthesis and characteristics of block copolymers (358 K, benzene, [monomer:solvent] = 1:3).

Block copolymerization					Characteristics of block copolymers			
Precursor	% per monomers	Monomer mixture	Polymerization rate $W \times 10^3$, %/s	Conversion, %	$[\eta] \times 10$, m^3/kg (298 K, acetone)	VEP link content, %	σ,* mN/m (10 % solution)	CMC**, %
VA-MP 95.5:4.5%	5.0	VA-VEP-N-VP 55:15:30	3.8	85	0.25	18	38.5	2.2
		VA-VEP-N-VP 20:35:45	1.3	75	0.15	42	32.0	1.5
	10.0	VA-VEP-N-VP 55:15:30	4.5	92	0.22	19	37.9	2.2
		VA-VEP-N-VP 20:35:45	2.2	85	0.13	40	32.2	1.7
VA-MA-MP 46:50:4.0	5.0	BA-VEP-GMA 30:55:15	5.8	98	0.10	63	–	
VA-BA-MP 25.1:70:4.9	5.0	BA-VEP-AA 35:40:25	7.1	98	0.10	50	33.5	3.0

*Surface tension.
**Critical concentration of micelle formation.

Synthesis of macro-initiators–precursors for graft copolymerization

Functional oligoperoxide initiators—precursors for graft copolymerization—were synthesized by copolymerization of VA with BA, MAN, or AA and unsaturated peroxide as monomer and chain-transfer agent simultaneously in hydrocarbon media and derived metal complexes on their basis, as referred [24]. Earlier, we showed [13] that OMCs are low-temperature macro-initiators of radical polymerization in hydrocarbon and water dispersion media, providing the obtainment of controlled graft copolymers of various backbone and side functional chains including groups of peroxide functionality. Some characteristics of OMC precursors are presented in Table 3.

Table 3 Characteristics of OMC precursors of graft (co)polymerization.

OMC composition, %					$[Cu^{2+}]$ in OMC, %	$[\eta] \times 10$, m^3/kg (298 K, acetone)	$\bar{M}_n$ g/mole	σ, mN/m (10 % solution at pH = 9)
VA	Vinyl alcohol	VEP	BA	MA				
18.4	–	50.6	–	31.0	0.85	0.08	1600	33.0
22.5	–	56.7	–	20.8	0.93	–	12 000	35.0
1.7	46.3	26.2	–	25.8	0.95	0.09	1800	35.0
1.6	56.1	17.8	24.5		0.35		1000	–
23.2	–	26.8	14.2	35.8	1.06	0.28	5200	30.0
10.6	–	15.8	60.1	13.5	1.25	–	14 300	

It is evident from Table 4 representing comb-like copolymer characteristics, that they contain different functional groups, including active ditertiary peroxide ones. One can see that obtained copolymers can be of controlled surface activity (Fig. 3), solubility, and reactivity, especially in the secondary processes of radical polymerization. Thus, grafting hydrophobic polystyrene chains to molecules of OMC initiator leads to the enhancement of the product surface activity in water-alkaline media; thereby, they can be used as radical-forming surfactants for synthesis of branched polymers and colloidal particles with predefined functionality and reactivity of the shell.

Table 4 Synthesis and characteristics of comb-like copolymers (358 K, benzene, [monomer: solvent] = 1:3).

Copolymerization					Characteristics of comb-like copolymers			
Precursor-initiator	OMC, % per monomers	Monomer mixture, %	Polymerization rate $W \times 10^3$ %/s	Conversion, %	$[\eta] \times 10$, m^3/kg (298 K, acetone)	Content of VEP links, %	σ, mN/m (10 % solution)	CMC, %
OMC VA-VEP-MA 20:48:32 % Cu^{2+} = 0.85%	2.5	AA-BA-VEP 90.0:5.0:5.0	0.08	60	0.095	8.0	35.0	5.0
		AA-N-VP-VEP 75.0:20.0:5.0	0.13	62	0.010	7.5	39.0	6.2
	5.0	AA-BA-VEP 90.0:5.0:5.0	0.17	65	0.090	8.6	37.0	5.2
		AA-N-VP-VEP 75.0:20.0:5.0	0.33	67	0.089	9.2	38.0	6.0

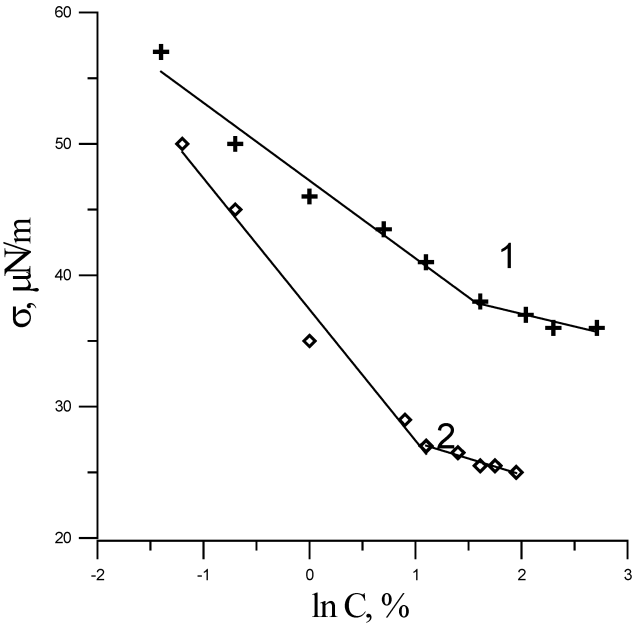

Fig. 3 Surface tension isotherms of OMC precursor (1) and comb-like OMC-graft-poly St (2) in water-ammonium solution.

The coincidence of characteristic absorption bands corresponding to Cu^{2+}-containing fragments in OMC molecules and derived comb-like copolymer testifies to structural entering of OMC residual fragments into the molecule of graft-copolymer obtained as a result of polymerization initiated by OMC precursor (Fig. 4).

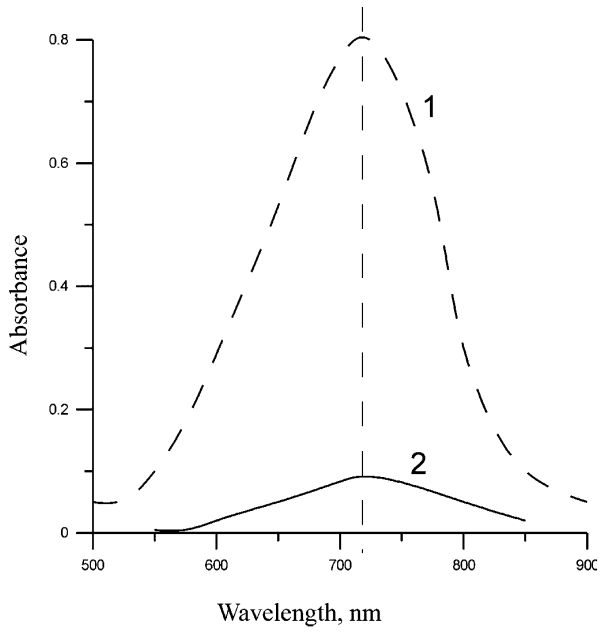

Fig. 4 UV–vis spectra of OMC (1) and OMC-graft-poly-St (2).

Comb-like copolymers containing radical-forming ditertiary peroxide fragments in the chains are prospective macro-initiators–precursors providing the obtainment of highly branched polymers. They initiate radical polymerization in the organic solutions in a wide temperature range, causing a formation of branched copolymers with new branches of tailored length, functionality, and reactivity (Table 5).

Table 5 Rheological characteristics (intrinsic viscosity) of OMC, copolymer OMC-graft-P1 and derived copolymer OMC-graft-P_1-graft-P_2.

Sample	$[\eta] \times 10$, m^3/kg (298 K, acetone)
OMC	0.082
Poly (VA-VEP-MA)-graft-poly (BA-VEP-AA)	0.090
Poly (VA-VEP-MA)-graft-poly (BA-VEP-AA)-graft-poly St	0.062

The rheological characteristics of polymer products that were obtained as a result of polymerization initiated by metal complexes on the basis of peroxide-containing macro-initiators of different degree of branching witness a formation in solution of new compact polymer structures peculiar to branched copolymer structure (Table 5).

Water dispersion polymerization initiated by OMCs

Previously, we [12,13] have studied the formation of primary reactive polymer nanoparticles with functional shell by the technique of water dispersion polymerization initiated by OMC. The main regularities of controlled radical polymerization initiated by oligoperoxide Me^{n+}-containing surfactants indicate a possibility of obtaining polymer water dispersions comprising of unimodal nanoparticles with particle size in the range of 30–70 nm, as shown in Fig. 5, and reactive functional shell capable of radical, condensation, and other reactions [13].

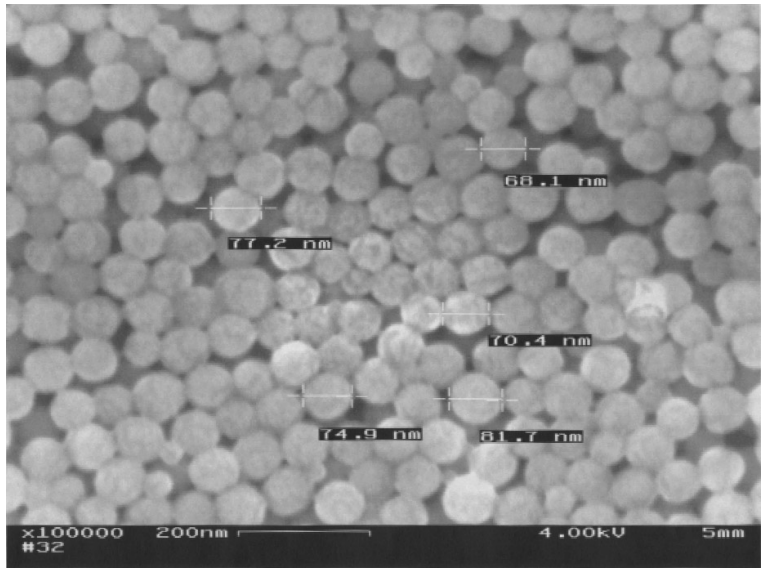

Fig. 5 SEM picture of functional polystyrene nanoparticles.

Using oligoperoxide-based coordinating complexes of cations of rare-earth elements for the initiation of St dispersion polymerization provides obtainment of luminescent polymeric nanoparticles with narrowed particle size distribution (Figs. 5 and 6).

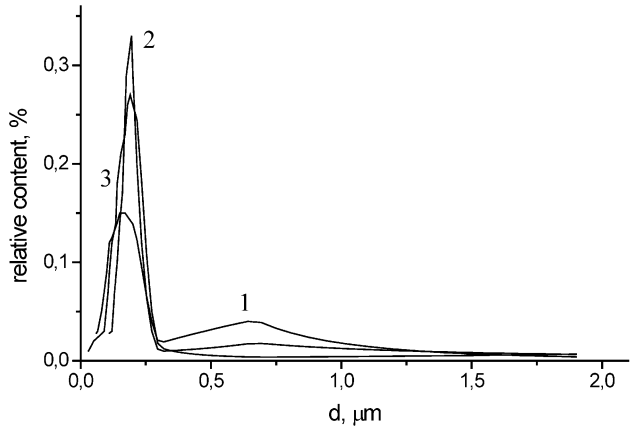

Fig. 6 Size distribution of luminescent polymeric nanoparticles: 1, polystyrene latex with 3 %; 2-polystyrene latex with 2 %; 3-polystyrene latex with 1 % of Ce^{3+} complex ($[Ce^{3+}]$ = 1.25 %).

One can see that highly monodisperse nanoparticles can be synthesized only at optimal content of luminescent OMC in water dispersion system, as initiator and stabilizer. That can be explained by the change of nanoparticle formation mechanism at different OMC concentrations.

As a result of sorption immobilization of luminescent SAP modifiers onto the magnetic ferric oxide nanoparticle surface, novel functional magnetic and luminescent nanoparticles were synthesized (Figs. 7 and 8).

Functional polystyrene nanoparticles possess an intensive luminescent capability due to the presence of coordinated Ce^{3+} cations in the functional particle shell. It is evident that a decrease of nanoparticle concentration in water system leads to an enhancement of luminescence intensity as a result of an increase of the system transparency (Fig. 8).

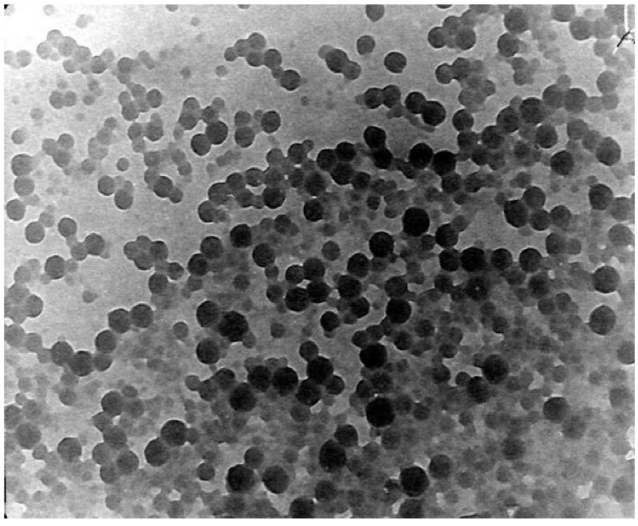

Fig. 7 TEM image of polystyrene nanoparticles with functional shell containing coordinated Ce^{3+} cations (2 % of Ce-oligoperoxide complex per H_2O, $[Ce^{3+}] = 1.25$ %).

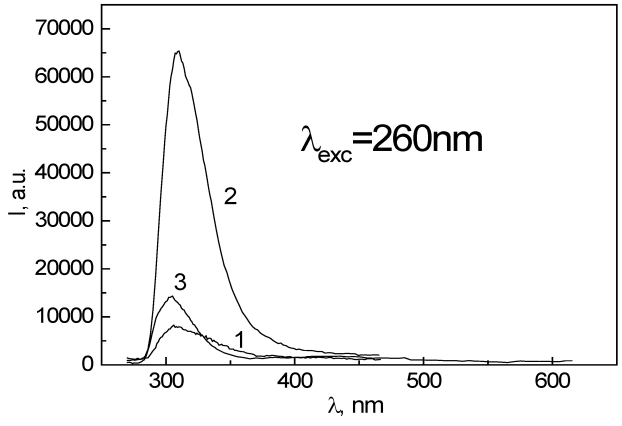

Fig. 8 Spectra of luminescence of polystyrene (1, 2) and hybrid magnetic (3) nanoparticles with functional shell containing Ce^{3+}-oligoperoxide complex. Polystyrene latex dry residue: 17 % (1); 2 % (2).

Seeded polymerization initiated from the surface of the particles modified by OMCs

Functional polymeric nanoparticles containing radical-forming sites in the oligoperoxide shell immobilized on the particle surface are efficient initiators of seeded polymerization providing grafting of various functional chains at a definite distance from the particle core. The experimental results of seeded low-temperature polymerization initiated from the surface of functional polymer nanoparticles are presented in Table 6. They display a formation of composite particles with "core-shell" morphology and a possibility of obtaining multilayer reactive shell. It is evident (Table 6) that various monomers and monomer systems can be used for the formation of second and third functional polymer shells on the particles resulting in changing particle hydrophobic–hydrophilic properties, functionality, and enhancement of their size.

Table 6 Multistage seeded copolymerization initiated from the particle surface (293 K).

First stage			Second stage*				Third stage**			
Latex particle structure	Dry residue, %	D_{part},, μm	Monomer for the second shell***	Dry residue, %	D_{part}, μm	Polymerization rate $W \times 10^3$, %/s	Monomer for the third shell	Dry residue, %	D_{part}, μm	Polymerization rate $W \times 10^3$, %/s
Core St-BA-VEP 53:32:15 Shell OMC	22.0	0.15	F-MA	27.0	0.020	20	–	–	–	–
			Si-MA	25.5	0.018	25	–	–	–	–
			BA-GMA 90:10	28.0	0.020	28	–	–	–	–
Core St-BA-AA 70:25:5 Shell - OMC	23.0	0.10	VEP-BA 50:50	29.0	0.014	25	Si-MA	33.0	0.16	20
							F-MA	32.2	0.16	25

*Formation of second shell was initiated by residual OMC in the particle shell.
**Formation of third shell was initiated by additional OMC sorbed onto that particle surface (0.5 % per monomers).
***F-MA: 2,2,3,3-tetrafluoropropyl-2-methacrylate; Si-MA: (3-trimethoxysilyl) propyl-2-methacrylate; GMA; (2,3-epoxy propyl)-methacrylate.

The study of seeded polymerization rate depending on the concentration of sodium pentadecyl sulfonate and particle-initiator content in the system, testifies to the polymerization occurrence exceptionally at the primary particle surface, providing an increase of their size. No particles are formed during seeded polymerization initiated by particles modified by OMCs.

As a result of seeded water dispersion polymerization initiated by radical-forming sites in functional oligoperoxide shell, novel particles with complicated morphology and targeted functionality, compatibility (including biocompatibility), and reactivity can be synthesized.

Homogeneous nucleation from salt solutions in the presence of SAPs or OMCs

The method of the formation of primary reactive inorganic particles with functional shell by homogeneous nucleation from the solutions of corresponding metal salts in the presence of SAPs and OMCs [24–26] is presented in Fig. 9. Reactive Ni colloids, Fe_3O_4, Ag, and other nanoparticles with narrowed particle size distribution and tailored functional shell and compatibility were synthesized by this technique in the presence of oligoperoxide surfactants [29–31]. The average particle size distribution testifies to a tendency of formation of unimodal nanoparticles at their formation in the presence of SAPs or OMCs (Fig. 10). That is explained, as we have shown earlier [12,13,29], by a displacement of the reaction of particle nucleation into micelle-like structures formed by functional oligoperoxide surfactants, which are the templates determining the particle size.

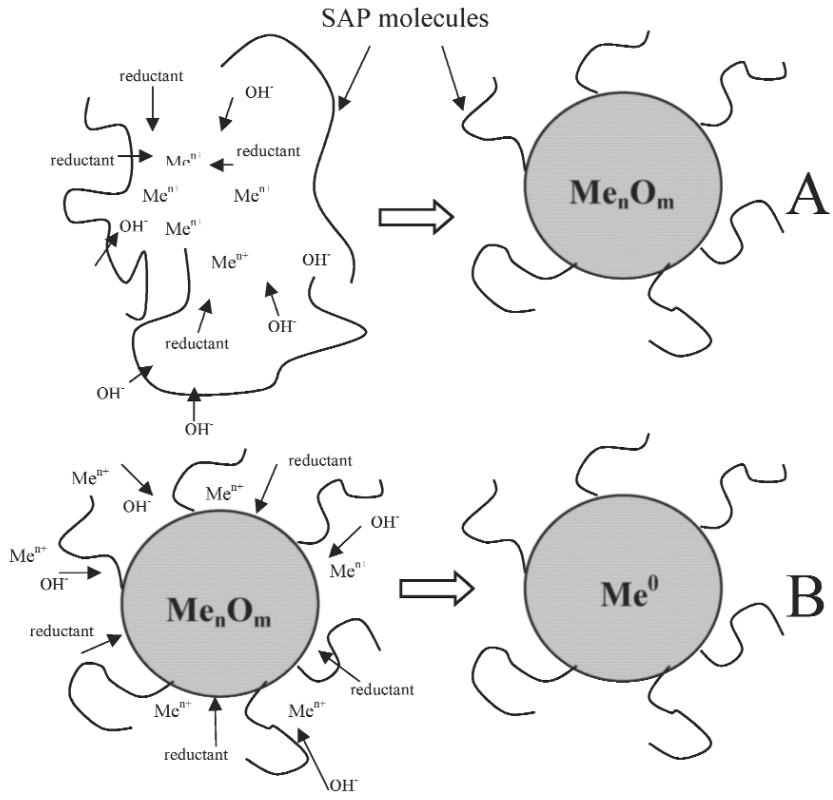

Fig. 9 Scheme of homogeneous nucleation of metal and metal oxide particles with functional SAP shell.

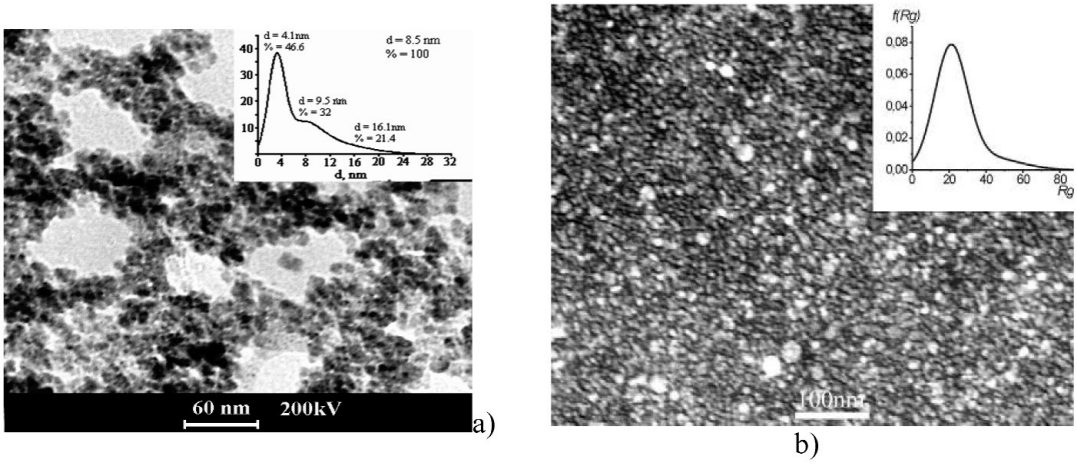

Fig. 10 Micrographs of functional hybrid nanoparticles obtained in the presence of SAP: (a) TEM image of magnetite crystals; (b) TEM image of colloidal silver particles (insets: number average distribution of particle size obtained from SAXS data).

TEM study of nanoparticle hydrosols (Fig. 10) witnesses a possibility of controlled synthesis of nanoparticles sized in the range of 5–20 nm depending upon the nature and content of SAPs and conditions of corresponding salt reduction in the presence of SAPs as template and stabilizer. SAXS tech-

nique (Table 7), TEM (Fig. 10), SEM, and magnetic measurements testify to favor of the realization of more complicated mechanism of ferric oxide formation as a result of homogeneous nucleation in the presence of functional oligoperoxide surfactants in accordance with the scheme (Fig. 11).

Table 7 Effect of synthesis temperature and SAP concentration on characteristics of functional magnetite nanoparticles.

T, K	[SAP], %	Crystal size, d_{cr}, nm	Polymer-mineral particle size d_N, nm	Polydispersity index k	Crystal amount per 1 particle, N*10^3
293	0	10.4 ± 1.0	146 ± 57	1.66	2.77
	0.2	9.6 ± 0.9	97 ± 27	4.62	1.03
	2	8.9 ± 0.9	78 ± 26	2.94	0.67
333	0	12.6 ± 1.1	71 ± 21	3.19	0.18
	0.2	10.5 ± 1.0	67 ± 19	2.21	0.26
	2	9.6 ± 0.9	–	–	–
363	0	13.3 ± 1.2	87 ± 39	1.83	0.28
	0.2	12.4 ± 1.1	72 ± 27	1.66	0.13
	2	10.2 ± 1.0	69 ± 27	2.14	0.47

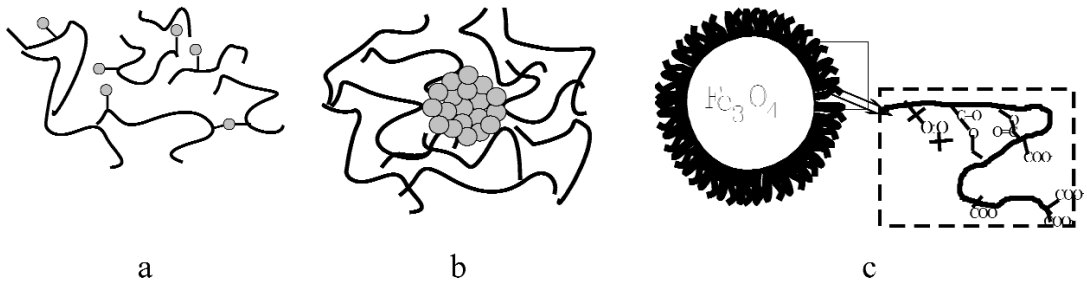

Fig. 11 Synthesis and transformation of biocompatible functional nanocarriers on the basis of Fe_3O_4.

Taking into account the results of SEM, TEM, and SAXS analysis, it can be suggested that integral Fe_3O_4 particles with size around 100–150 nm comprised of magnetic mineral core containing nanocrystals sized 8–12 nm with functional polymeric shell providing radical reactions initiated at the particle surface. SAP concentration and temperature of synthesis are the main factors determining integral nanoparticle size, as well as the size of nanocrystals (Table 7). TEM micrographs of magnetite nanoparticles after sonification during 4 and 40 s confirm complicated Fe_3O_4 nanoparticle morphology (Fig. 12).

The availability of reactive functional shell on the nanoparticle surface not only provides tailored rheological characteristics and compatibility with various matrixes, but also indicates a possibility of occurrence of radical and other reactions with participation of functional fragments located in the particle shell.

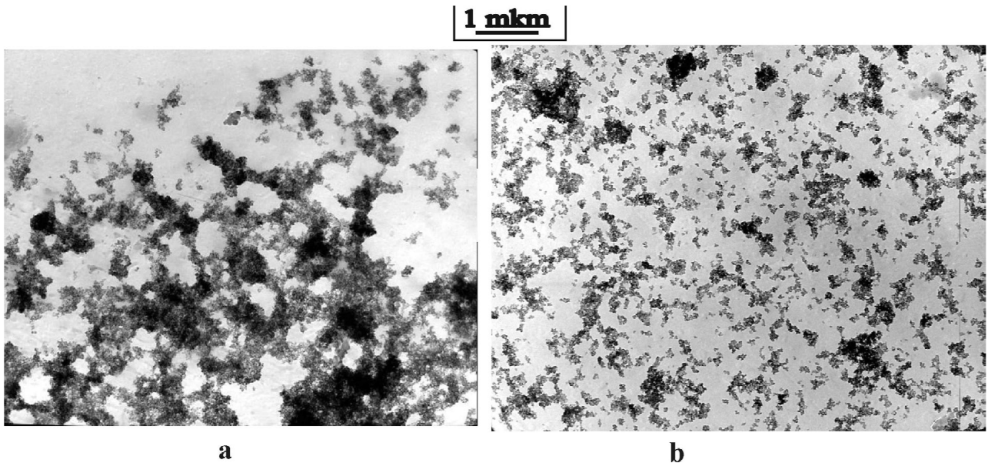

Fig. 12 TEM images of Fe_3O_4 nanoparticles after 4 s (a) and 40 s (b) ultrasound treatment.

Seeded polymerization initiated from inorganic particle surface modified by OMCs

The availability of radical-forming sites on the particle surface causes a possibility of radical formation by immobilized ditertiary peroxide groups and grafting polymer chains to surface with following formation of new functional shell at a given distance from the surface (Fig. 13 and Table 8). As one can see (Fig. 13), seeded polymerization initiated from the surface of inorganic particles obeys the same regularities that are peculiar for polymerization initiated from the polymer particle surface, including independence on the concentration of the added emulsifier. That proves an occurrence of graft polymerization only on the particle surface and the impossibility of particle formation in the medium. The polymerization rate and conversion depend strongly on the modified filler nature and content in the reaction system. The study of the particles after seeded polymerization witnesses an increase of their size and tailored formation of grafted chains containing the definite amount of active functional fragments.

Table 8 Characteristics of copolymer GMA-VEP-St grafted to the surface of inorganic nanoparticles (291 K; monomers: H_2O = 1:5; GMA-VEP-St = 2:1:1).

Particles	Particle content, %	Content of grafted copolymer, %	Composition of copolymer grafted, %		
			GMA	VEP	St
γ-Fe_2O_3, [OMC] = 0.7 %	17.4	1.6	50.0	25.0	25.0
	30	2.5	60.0	19.0	21.0
	60	5.0	75.0	16.0	9.0
Colloidal Ni [OMC] = 0.45 %	17.4	0.8	65.0	5.5	29.5
	30	1.1	55.0	6.0	39.0
	60	2.5	50.0	10.0	40.0

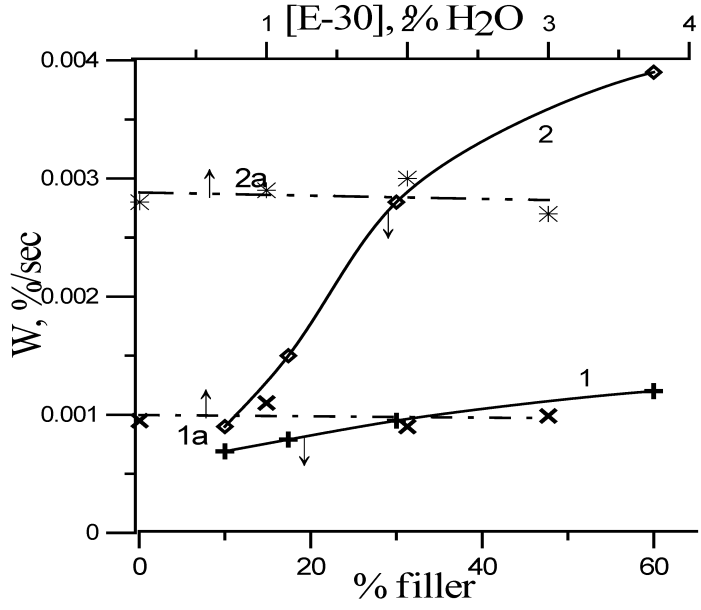

Fig. 13 Water dispersion polymerization rate of VEP-GMA-St mixture vs. filler content (1, 2) and concentration of emulsifier E-30 (1a, 2a). Initiation from the OMC-modified filler surface: γ-Fe_2O_3 ([OMC] = 0.7 %) (1, 1a) colloidal Ni particles ([OMC] = 0.45 %) (2, 2a); 291 K.

Potentials for biomedical application: Employment of nanoparticles in studying phagocytic activity

Latex nanoparticles were pretreated with different proteins and these particles were further used as objects of phagocytosis. It is known that the efficiency of ingestion of particles by phagocytic mammalian cells (neutrophilic granulocytes or macrophages) depends upon properties of particle surface, especially upon proteins located at the surface. Substances, including proteins, which stimulate phagocytosis are called "opsonins", and the process of particle coating with these substances is called "opsonization". Immunoglobulins and antibodies immobilized on the particle surface by different bonds (physical or chemical) are the most effective opsonins.

We used proteins of human blood serum or concanavalin A for opsonization of nanoparticles. Concanavalin A is a plant lectin, which is a protein that selectively binds carbohydrates, such as mannose, glucose, and acetamidoglucose. In natural conditions, it binds polysaccharides (glucans and mannans) or glycoproteins exposing residues of mannose and acetamidoglucose. Concanavalin A absorbed on that nanoparticle surface favors the particle attachment to cell surface and its engulfment during phagocytes. An example of cytological pattern of phagocytosis of different opsonized nanoparticles, including polymer-coated nickel particles, is presented in Fig. 14.

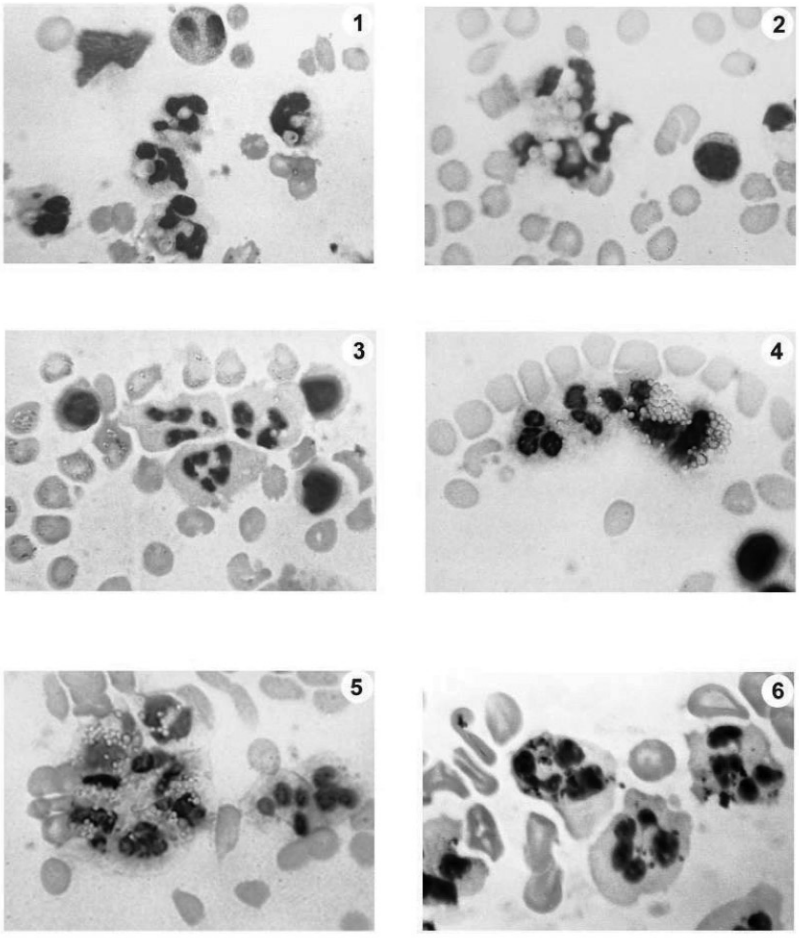

Fig. 14 Phagocytic activity of human blood polymorphonuclear leukocytes toward different nanosized objects of phagocytosis. (1, 2) phagocytosis of yeast *Debariomyces hansenii* cells; (3–5) nanoparticles used as objects of phagocytosis: (3) Ni nanoparticles opsonized with proteins of human blood serum; (4) latex nanoparticles opsonized with proteins of human blood serum; (5) latex nanoparticles opsonized with lectin concanavalin A; (6) nickel nanoparticles coated with a polymeric shell.

CONCLUSIONS

The principal possibility of using peroxide-containing monomer or telogen, as well as surface-active polymeric substances on their basis, for tailored design of reactive macromolecules of block, comb-like, and branched structure with peroxide-containing chains of various nature, HLB, and reactivity was demonstrated.

The results of studying kinetic peculiarities and other characteristics of novel designed copolymers displayed that they are surface-active substances with controlled solubility, rheological characteristics, surface activity, and capability of radical formation in a wide temperature range.

Various approaches of using oligoperoxide-based surfactants including derived coordinating metal complexes for the activation of colloidal particles causing polymer grafting onto their surface have been demonstrated. That permits obtaining of nanoparticles of "core-shell" structure with fragments providing their tailored compatibility, functionality, and reactivity including biocompatibility and specific biological activity.

Functional nanoparticles, including magnetic, colored and luminescent ones, were successfully used as stained or magnetic labels for investigation of phagocytosis, labeling pathological cells, as well as nanocarriers for targeted drug delivery. The advantages of using polymeric nanoparticles comparing to yeast cells, possibilities of chemical conditioning of the particle surface and its modification by attaching specific ligands with known structure can be clearly seen in phagocytosis experiments. Proposed technology of latex nanoparticle synthesis and fractionation for obtaining monodisperse suspensions can be used for measuring phagocytic activity of human blood cells for the diagnostic purposes in clinical laboratories.

ACKNOWLEDGMENTS

We thank prof. A. Voloshinovsky (Lviv National University), prof. M. Lootsik (Institute of Cell Biology, Lviv, Ukraine) for helpful discussions and practical support. We grateful to Dr A. Bilyy for measurements of polystyrene particle size.

REFERENCES

1. J. H. Park, K. H. Park, D. P. Kim. *J. Ind. Eng. Chem.* **13**, 27 (2007).
2. P. Baldus, M. Jansen, D. Spoorn. *Science* **285**, 699 (1999).
3. C. Park, J. Yoon, E. L. Thomas. *Polymer* **44**, 6725 (2003).
4. C. Harrison, P. M. Chaikin, R. A. Register, D. H. Adamson. *Science* **276**, 1401 (1997).
5. R. A. Segalman. *Mater. Sci. Eng.* **48**, 191 (2005).
6. S. K. Alahari, R. DeLong, M. H. Fisher, N. M. Dean, R. L. Juliano. *J. Pharm. Exp. Ther.* **286**, 419 (1998).
7. M. Ruponen, S. Yla-Herttuala, A. Urtti. *Biochem. Biophys. Acta* **1415**, 331 (1999).
8. U. Boas, P. M. H. Heegaard. *Chem. Soc. Rev.* **33**, 43 (2004).
9. D. A. Tomalia, A. M. Naylov, W. A. Goddard. *Angew. Chem., Int. Ed. Engl.* **29**, 138 (1990).
10. J. Issberner, R. Moors, F. Votle. *Angew. Chem., Int. Ed. Engl.* **33**, 2413 (1994).
11. G. R. Newkome, A. Mishra, C. N. Moorefield. *J. Org. Chem.* **67**, 3957 (2002).
12. A. Zaichenko, N. Mitina, O. Shevchuk, O. Hevus, T. Kurysko, N. Bukartyk, S. Voronov. *Macromol. Symp. (React. Pol.)* **164**, 25 (2001).
13. A. Zaichenko, N. Mitina, M. Kovbuz, I. Artym, S. Voronov. *Macromol. Symp. (React. Pol.)*. **164**, 47 (2001).
14. A. P. Alivisatos. *Science* **271**, 933 (1996).
15. J. Zhu, F. Xu, S. J. Schofer, C. A. Mirkin. *J. Am. Chem. Soc.* **119**, 235 (1997).
16. J. J. Storhoff, R. Elghanian, R. C. Mucic, C. A. Mirkin, R. L. Letsinger. *J. Am. Chem. Soc.* **120**, 1959 (1998).
17. C. R. Mayer, S. Neveu, V. Cabuil. *Angew. Chem., Int. Ed.* **41**, 501 (2002).
18. D. A. Tomalia, P. R. Dvornic. *Nature* **372**, 617 (1994).
19. Y. Wang, N. Toshima. *J. Phys. Chem.* **101**, 5301 (1997).
20. M. Antonietti, E. Wenz, L. Bronstein, M. Seregina. *Adv. Mater.* **7**, 1000 (1995).
21. S. Rimmer. *Designed Monom. Polym.* **1**, 89 (1998).
22. M. Okubo, R. Takekoh, H. Sugano. *Colloid Polym. Sci*. **278**, 559 (2000).
23. A. Zaichenko, S. Voronov, A. Kuzayev, O. Shevchuk, V. Vasilyev. *J. Appl. Polym. Sci.* **70**, 2449 (1998).
24. A. Zaichenko, N. Mitina, M. Kovbuz, L. Artym, S. Voronov. *J. Polym. Sci., Part A: Polym. Chem.* **38**, 516 (2000).
25. A. Zaichenko, S. Voronov; O. Shevchuk. UA Patent 20068A, Filed 07 July 1995, Issued 25 Dec. 1997.

26. A. Zaichenko, I. Bolshakova, N. Mitina, O. Shevchuk, A. Bily, V. Lobaz. *J. Magn. Magn. Mater.* **289**, 17 (2005).
27. V. P. Vasilyev. Ph.D. thesis, Lviv Polytechnic National University (1990).
28. A. M. Toroptseva, K. V. Belogorodskaya, V. M. Bondarenko. *Laboratory Training on Chemistry and Technology of High Molecular Substances*, p. 384, Khimiya, Leningrad (1972).
29. A. Zaichenko, O. Shevchuk, V. Samaryk, S. Voronov. *J. Colloid Interface Sci.* **275**, 204 (2004).
30. V. Novikov, A. Zaichenko, N. Mitina, O. Shevchuk, K. Raevska, V. Lobaz, V. Lubenets, Yu. Lastukhin. *Macromol. Symp.* **210**, 193 (2004).
31. A. Zaichenko, O. Shevchuk, S. Voronov, A. Sidorenko. *Macromolecules* **32**, 5707 (1999).